*The Plant Journal* (2005) **41**, 831–844 doi: 10.1111/j.1365-313X.2005.02346.x

# Senescence-associated vacuoles with intense proteolytic activity develop in leaves of Arabidopsis and soybean

**Marisa S. Otegui[1,2,*], Yoo-Sun Noh[3,†], Dana E. Martínez[1], Martin G. Vila Petroff[4], L. Andrew Staehelin[5], Richard M. Amasino[3] and Juan J. Guiamet[1]**

[1]*Instituto de Fisiología Vegetal (INFIVE), Universidad Nacional de La Plata, c.c. 327, 1900, La Plata, Argentina,*
[2]*Department of Botany, University of Wisconsin, 430 Lincoln Drive, Madison, WI 53706, USA,*
[3]*Department of Biochemistry, University of Wisconsin, 433 Babcock Drive, Madison, WI 53706, USA,*
[4]*Centro de Investigaciones Cardiovasculares, Facultad de Ciencias Médicas, Universidad Nacional de La Plata, 1900, La Plata, Argentina, and*
[5]*Department of Molecular, Cellular, and Developmental Biology, University of Colorado, Boulder, 347 UCB, CO 80309-0347, USA*

Received 13 September 2004; revised 6 December 2004; accepted 10 December 2004.
*For correspondence (fax +608 262 7509; e-mail otegui@wisc.edu).
†Present address: Kumho Life & Environmental Science Laboratory, 1 Oryong-Dong, Puk-Gu, Kwangju 500-712, South Korea.

**Summary**

**Vacuolar compartments associated with leaf senescence and the subcellular localization of the senescence-specific cysteine-protease SAG12 (senescence-associated gene 12) were studied using specific fluorescent markers, the expression of reporter genes, and the analysis of high-pressure frozen/freeze-substituted samples. Senescence-associated vacuoles (SAVs) with intense proteolytic activity develop in the peripheral cytoplasm of mesophyll and guard cells in Arabidopsis and soybean. The vacuolar identity of these compartments was confirmed by immunolabeling with specific antibody markers. SAVs and the central vacuole differ in their acidity and tonoplast composition: SAVs are more acidic than the central vacuole and, whereas the tonoplast of central vacuoles is highly enriched in γ-TIP (tonoplast intrinsic protein), the tonoplast of SAVs lacks this aquaporin. The expression of a SAG12-GFP fusion protein in transgenic Arabidopsis plants shows that SAG12 localizes to SAVs. The analysis of *Pro$_{SAG12}$:GUS* transgenic plants indicates that *SAG12* expression in senescing leaves is restricted to SAV-containing cells, for example, mesophyll and guard cells. A homozygous *sag12* Arabidopsis mutant develops SAVs and does not show any visually detectable phenotypical alteration during senescence, indicating that SAG12 is not required either for SAV formation or for progression of visual symptoms of senescence. The presence of two types of vacuoles in senescing leaves could provide different lytic compartments for the dismantling of specific cellular components. The possible origin and functions of SAVs during leaf senescence are discussed.**

**Keywords: cellular breakdown, SAG12, senescence, senescence-associated protease, vacuoles.**

## Introduction

Leaf senescence is a highly regulated developmental process that ends with the programmed death of leaf cells (Swidzinski *et al.*, 2002). During leaf senescence, cellular components such as proteins, lipids, and nucleic acids are degraded, and the released nutrients are mobilized from the leaves for re-use in other parts of the plant (Lim *et al.*, 2003; Noodén and Guiamet, 1996; Quirino *et al.*, 2000). The levels of most proteins drop substantially during this process whereas representatives of the major classes of proteases, cysteine (Cys)-, aspartic-, serine-, and metallo-proteases, increase in activity, concentration, or expression at the transcript level (Buchanan-Wollaston and Ainsworth, 1997; Drake *et al.*, 1996; Lin and Wu, 2004; Nakabayashi *et al.*, 1999; Smart *et al.*, 1995; Weaver *et al.*, 1998).

*SAG12* is one of the senescence-associated genes identified in Arabidopsis (Lohman *et al.*, 1994). This gene encodes a senescence-specific papain-like Cys-protease, and studies of the *SAG12* promoter (*Pro$_{SAG12}$*) have shown

 

it to be tightly regulated during leaf senescence (Gan and Amasino, 1995; Noh and Amasino, 1999a,b). The cellular location of most of the senescence-associated proteases is unknown (Buchanan-Wollaston, 1997). Paradoxically, whereas chloroplasts contain most of the leaf protein, subcellular fractionation studies indicate that most of the proteolytic activity in senescing leaf cells is located elsewhere, particularly in the vacuole (Feller and Fisher, 1994; Wittenbach *et al.*, 1982). Moreover, vacuolar processing enzymes, an important subset of Cys-proteases that are involved in maturation of vacuolar proteins, are also upregulated during senescence (Kinoshita *et al.*, 1999; Smart *et al.*, 1995), suggesting an important role for the vacuole in protein degradation during senescence, as originally suggested by Matile (1975).

The central vacuole is the largest lytic compartment in the mature plant cell and it contains most of the cellular hydrolytic activity (e.g., 80–100% of acid protease and 50–100% of acid nuclease activities; De, 2000). It is not known whether the central vacuole is involved in the breakdown of cellular components such as chloroplasts, mitochondria or cytosolic proteins, as part of the nutrient remobilization program during senescence, although there have been claims of chloroplast engulfment within the central vacuoles of both senescing bean (Minamikawa *et al.*, 2001) and wheat leaf cells (Wittenbach *et al.*, 1982).

Interestingly, several types of vacuoles, with different contents and tonoplast composition, may coexist within a single cell (Jauh *et al.*, 1999; Swanson *et al.*, 1998). Recent studies based on the expression of the green fluorescent protein (GFP) fused to different vacuolar sorting peptides, have shown that, in addition to the large central vacuole, there is a population of small, peripheral vacuoles in tobacco mesophyll protoplasts (Di Sansebastiano *et al.*, 2001; Neuhaus, 2000). In addition, the vacuolar membrane $Ca^{2+}$ pump ACA4 (Arabidopsis $Ca^{2+}$ ATPase 4) fused to GFP localizes to small peripheral vacuoles in Arabidopsis protoplasts, but not to the tonoplast of the central vacuole (Geisler *et al.*, 2000).

How these functionally different vacuoles arise and differentiate is not completely understood. In many cases, autophagic mechanisms appear to be responsible for *de novo* formation of vacuolar compartments in plants (Moriyasu and Hillmer, 2000; Robinson and Hinz, 1997). Autophagy is a ubiquitous eukaryotic process by which cytoplasm and organelles can be internalized into vacuoles for degradation. Several orthologs of yeast *APG* (*AUTOPHAGIC GENES*) genes have been found in Arabidopsis, and the importance of autophagic mechanisms during leaf senescence has become evident (Doelling *et al.*, 2002; Hanaoka *et al.*, 2002). The expression of *AtAPG7* has been shown to increase during senescence of detached leaves (Doelling *et al.*, 2002), and *atapg7* and *atapg9* mutants display an accelerated senescence phenotype, particularly under conditions of nutrient starvation (Doelling *et al.*, 2002; Hanaoka *et al.*, 2002).

In this study, we have chosen two monocarpic species, *Arabidopsis thaliana* and soybean, to examine the subcellular localization of the proteolytic activity associated with leaf senescence. We have found that during senescence a population of small, lytic vacuoles (approximately 550–700 nm in diameter) develops in the peripheral cytoplasm of leaf cells that contain chloroplasts. The analysis of transgenic Arabidopsis plants containing a $Pro_{SAG12}$:*SAG12-GFP* construct shows that the SAG12-GFP fusion protein localizes to these small senescence-associated vacuoles (SAVs). The expression of the reporter gene β-glucuronidase (GUS) under the control of the $Pro_{SAG12}$ indicates that SAG12 expression in leaves is restricted to SAV-containing cells. In addition, we show that the SAVs are more acidic than the central vacuole, and that both types of vacuoles differ in tonoplast composition.

## Results

### *A population of small acidic compartments with intense proteolytic activity develop during leaf senescence*

Based on the degree of expansion and chlorophyll content we defined five developmental stages for both Arabidopsis and soybean leaves (Figure 1). Leaves at stages S1, S2, S3 showed increasing loss of chlorophyll (30–50%, 50–75%, and more than 75%, respectively, relative to NS2 leaves) and were considered senescent.

In order to identify cellular compartments with high proteolytic activity during senescence, we incubated isolated cells and protoplasts from NS1 to S3 soybean and Arabidopsis leaves in R-6502 (rhodamine 110, bis-CBZ-L-phenylalanyl-L-arginine amide) (Figure 2). R-6502 is a rhodamine 110-based substrate for Cys-proteases that become brightly fluorescent upon hydrolysis of the two amide moieties. Isolated cells and protoplasts were used instead of leaf pieces to facilitate the incorporation of the dye into the leaf cells. In R-6502-treated S1, S2, and S3 leaf cells of soybean and Arabidopsis, there was an intense punctuate fluorescent pattern (Figure 2f,n). These fluorescent structures were approximately 0.7 μm in diameter and were located in the peripheral cytoplasm, around plastids (Figure 2h,p). No such structures were observed in cells from NS1 and NS2 leaves incubated in the same reagent (Figure 2b,j). In addition, the protease substrate R-6502 was also loaded and hydrolyzed in the central vacuole of senescing and non-senescing leaf cells, but here the fluorescence signal was very dim (data not shown).

To determine the identity of the small organelles that appear to contain most of the Cys-protease activity in senescing leaf cells, we co-incubated isolated leaf cells and protoplasts with R-6502 and Lysotracker Red or Neutral Red,

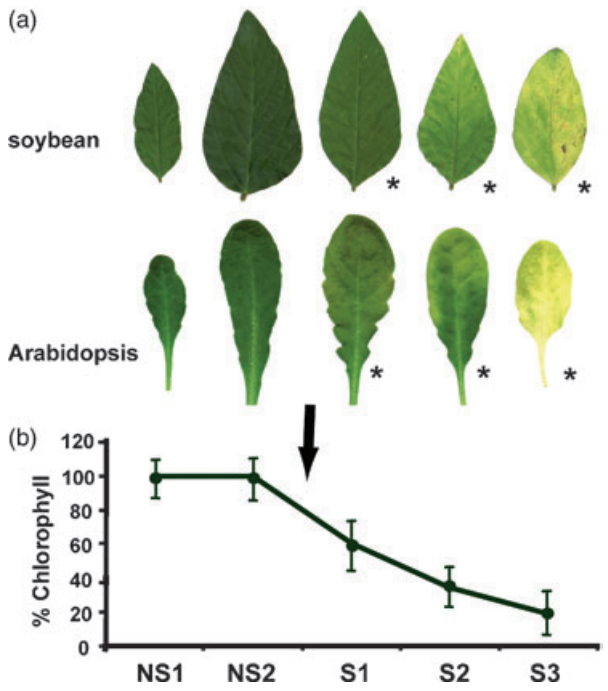


**Figure 1.** General aspect of soybean leaflets and *Arabidopsis thaliana* leaves during development correlated with chlorophyll content.
(a) Developmental stages: NS1, non-senescing, partially expanded leaflet/leaf; NS2, non-senescing, fully expanded leaflet/leaf; S1, 30–50% loss of chlorophyll (relative to NS2 leaves); S2, 50–75% chlorophyll loss; S3, more than 75% chlorophyll loss. Asterisks indicate those stages in which senescence-associated vacuoles were observed. Arrow points out the developmental stage in which SAVs develop.
(b) Changes in chlorophyll content during leaf development. All values were based on three chlorophyll meter readings made at the center of the leaves with a Minolta SPAD-502 chlorophyll meter and expressed as percentage of chlorophyll content in non-senescing leaves.

both of which are fluorescent markers for acidic organelles such as lysosomes and vacuoles (Di Sansebastiano *et al.*, 2001; Toyooka *et al.*, 2001). We found that the fluorescence signal from the hydrolyzed R-6502 co-localizes with both Lysotracker Red and Neutral Red, suggesting that the Cys-protease activity identified in senescing leaf cells is confined to acidic vacuolar compartments (Figure 2g,h,o,p).

Electron microscopy of high-pressure frozen/freeze-substituted senescing and non-senescing leaves of soybean and Arabidopsis confirmed that small vacuolar compartments of approximately 550–700 nm in diameter appear in the cytoplasm of senescing mesophyll cells (Figure 3a–c). As shown in the next section (see below), these organelles contain vacuolar markers, confirming they are indeed vacuolar compartments, and we have called them SAVs. SAVs often contain dense aggregates in their lumen which may consist of partially degraded cellular material (Figure 3a–c), similar in appearance to the contents of late autophagic vacuoles described in other eukaryotic cells (Eskelinen *et al.*, 2002). However, in the few cases where characteristic intermediates in autophagosome formation were evident, for example, portions of cytoplasm enclosed by a membranous structure (Figure 3d), they were much larger than the senescence-associated compartments, which suggests that SAVs do not derive from these autophagosomes. Based on serial section analysis, we have determined that SAVs are not connected with the central vacuole (data not shown).

### *Immunolocalization of vacuolar markers in senescing leaf cells*

In order to confirm the vacuolar identity of the senescence-associated organelles we performed immunolocalization studies on plastic sections of high-pressure frozen/freeze-substituted Arabidopsis senescing leaves. The polyclonal antibody against the Arabidopsis vacuolar ($H^+$)-pyrophosphatase labeled the membranes of both the central vacuole and SAVs (Figure 4a,b), clearly indicating that these senescence-associated organelles are indeed vacuoles. To determine if SAVs contain markers for lytic vacuoles, we used the polyclonal antibody against radish TIP-VM23 (Maeshima, 1992), a member of the $\gamma$-TIP subfamily of aquaporins (Paris *et al.*, 1996). The antibody heavily labeled the tonoplast of the central vacuole but did not label the SAV membrane (Figure 4c).

### *SAG12-GFP localizes to the SAVs*

We expressed *SAG12*, which encodes a leaf senescence-specific Cys-protease (Lohman *et al.*, 1994), fused to *GFP* under the control of the $Pro_{SAG12}$ in Arabidopsis plants (Figure 5). No GFP signal was detected in non-senescing leaves (NS1 and NS2, data not shown), whereas in senescing leaves (S1–S3), the GFP fluorescence was present in a punctuate pattern (Figure 5b) similar to that observed in senescing leaf cells incubated with the protease substrate R-6502. Moreover, the GFP fluorescence co-localizes with Lysotracker Red (not shown) and Neutral Red (Figure 5c,d), indicating that SAG12-GFP localizes to the SAVs previously identified with R-6502.

The intensity of the GFP fluorescence in the SAVs was in general quite low. Because GFP targeted to certain plant vacuoles can be degraded by proteases in a light-dependent manner (Tamura *et al.*, 2003), we also evaluated SAG12-GFP transgenic plants kept in the dark for 24 h. However, no change in the intensity of the GFP signal was detected. No GFP signal was observed in the central vacuoles of senescing leaf cells, even in samples from plants kept in the dark for 24 h.

### *SAV formation and SAG12 expression occur coincidentally in mesophyll and guard cells*

In order to determine if all leaf cells develop SAVs, we incubated small pieces of Arabidopsis S1 and S2 leaves in

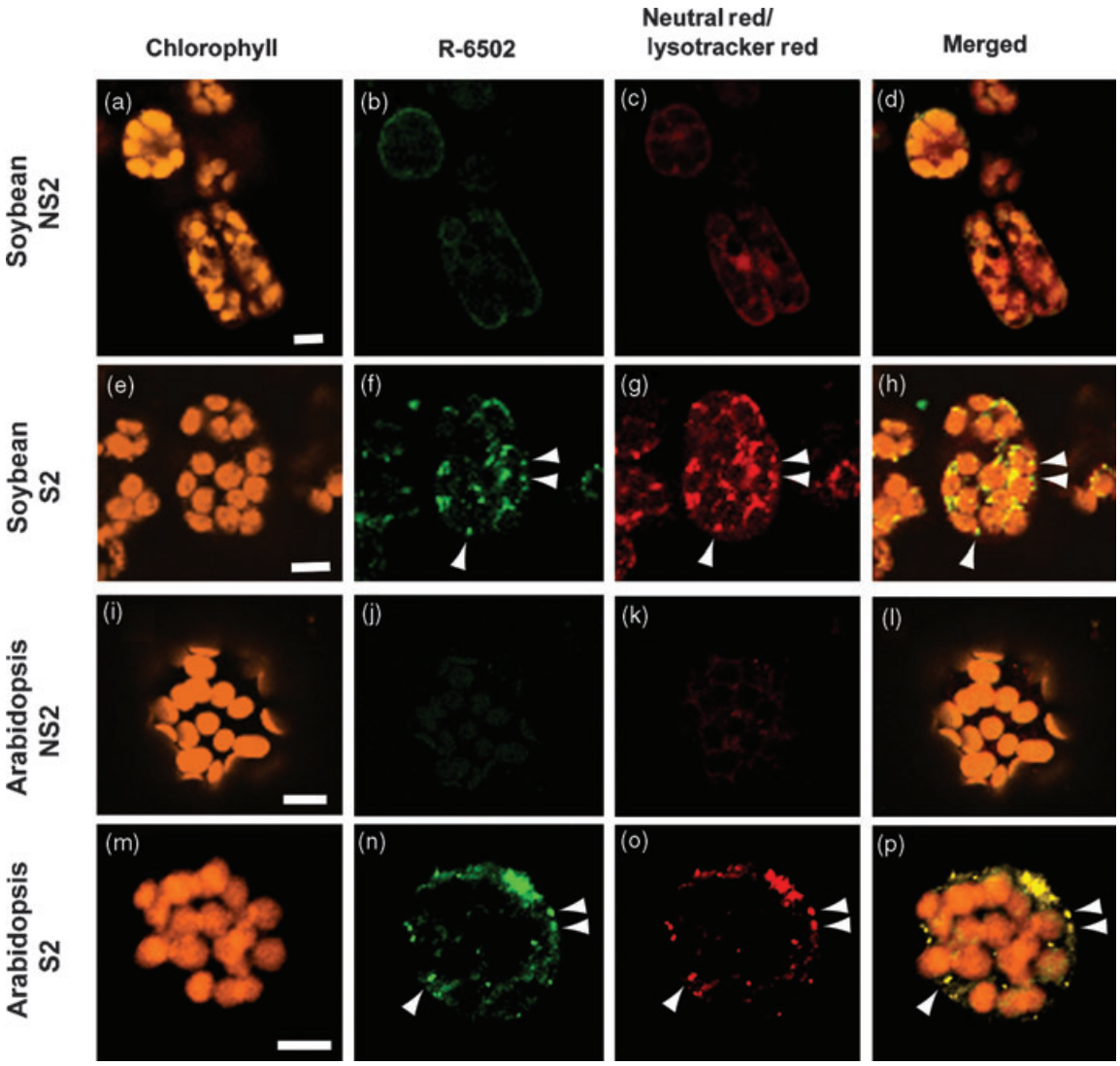


**Figure 2.** Senescence-associated vacuoles (SAVs) in isolated leaf cells and protoplasts from soybean and Arabidopsis.
Samples were labeled with R-6502 and Neutral Red (b, c, f, g) and with R-6502 and Lysotracker Red (j, k, n, o). Note that the R-6502 fluorescent signal colocalizes with the Lysotracker Red/Neutral Red signal (h, p). Confocal sections were obtained through the cortical cytoplasm of leaf cells and protoplasts.
(a–d) Isolated cells from non-senescing (NS2) soybean leaves.
(e, h) Isolated cells from senescing (S2) soybean leaves; note the punctuate pattern corresponding to SAVs (arrowheads).
(i–l) Protoplasts from non-senescing (NS2) Arabidopsis leaves.
(m–p) Protoplasts from senescing (S2) Arabidopsis leaves; note the punctuate pattern corresponding to SAVs (arrowheads).
Scale bars = 10 μm.

Lysotracker and Neutral Red. In both cases, we observed that SAVs develop in mesophyll and guard cells but not in the remaining epidermal cells (Figure 6).

To determine if SAG12 expression is confined to those leaf cells that form SAVs, we analyzed the expression pattern of both SAG12-GFP and GUS under the control of the $Pro_{SAG12}$. As noted above, the GFP signal from SAVs was often difficult to observe. However, the GUS expression pattern clearly indicates that SAG12 is exclusively expressed in mesophyll and guard cells of senescing leaves (S1–S3 leaves), and not in other epidermal cells (Figure 7).

### *The central vacuole and the SAVs differ in their intravacuolar pH*

We compared the lumenal pH of both SAVs and central vacuoles in senescing leaves by using the acidotropic fluorescent probe Lysosensor Yellow/Blue DND-160. This probe has been shown to be sequestered into vacuolar (Swanson *et al.*, 1998) and lysosomal compartments (Diwu *et al.*, 1999; Holopainen *et al.*, 2001), and to exhibit both dual-excitation and dual-emission spectral peaks that are pH-dependent (Diwu *et al.*, 1999). We used this probe as a

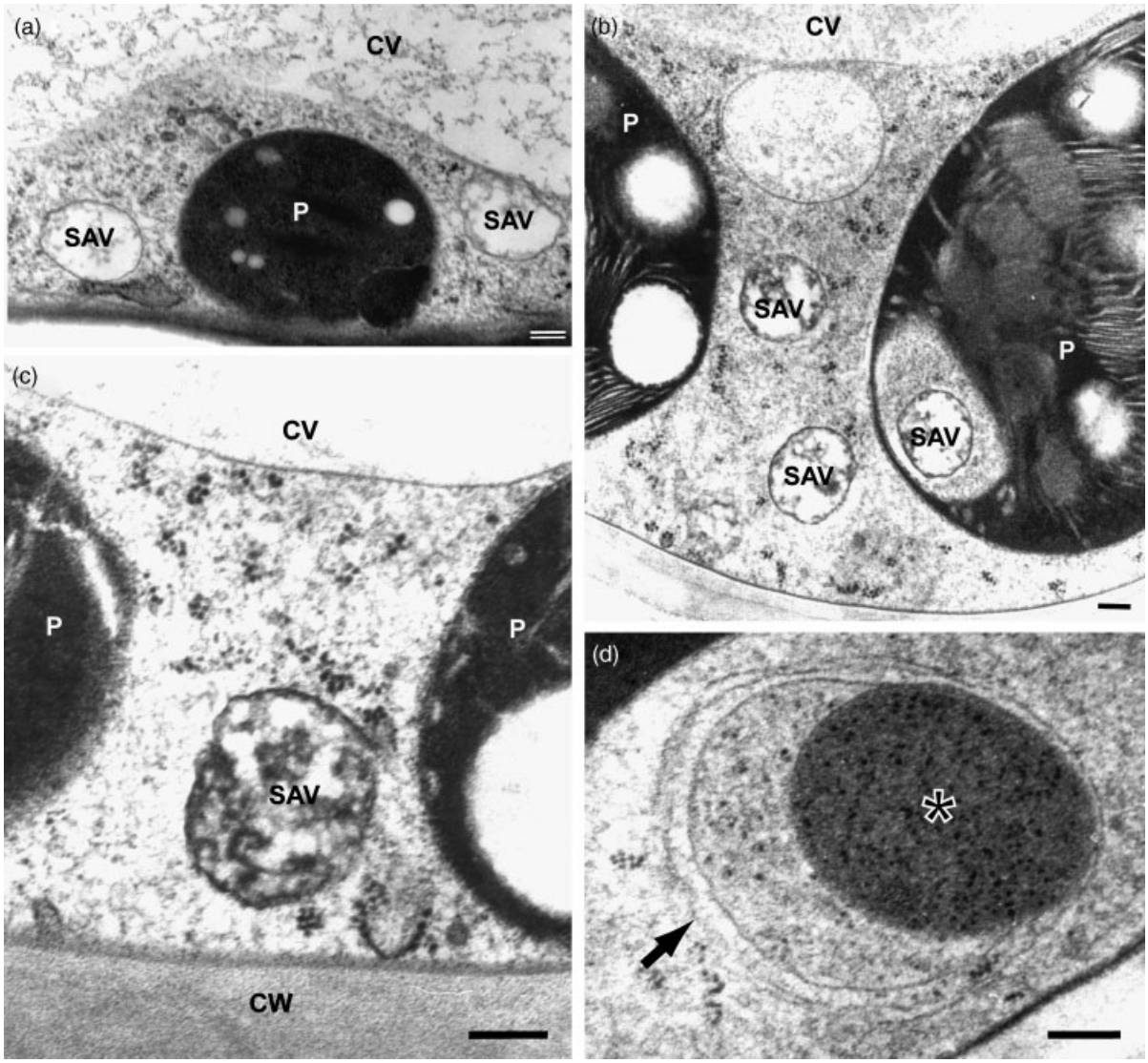


**Figure 3.** Electron micrographs of senescing leaves.
(a) Senescing Arabidopsis leaf cell. Senescence-associated vacuoles (SAVs) have developed in the peripheral cytoplasm surrounding the central vacuole (CV), P, plastid.
(b) Senescing soybean leaf cell showing the presence of SAVs in addition to the central vacuole (CV). The SAV on the right and the surrounding cytoplasm are partially trapped by a P (plastid) evagination.
(c) SAV with dense contents located in the peripheral cytoplasm of a senescing soybean leaf cell, between two plastids (P). Note the different appearance of the lumenal contents of SAV and CV.
(d) Autophagosome-like structure surrounded by a membranous structure (arrow) and enclosing cytoplasm and a ribosome-containing organelle, likely a plastid or a plastid-derived structure (asterisk).
Scale bars in (a) and (b) = 200 nm.

pH indicator measuring its ratio of fluorescence emission at two excitation wavelengths; therefore, the ratio values were independent of fluorescence intensity variations due to vacuole size and/or concentration of the probe inside cellular compartments. The calibration curve was performed by measuring leaf protoplasts labeled with Lysosensor Yellow/Blue and treated with the protonophore nigericin in calibration buffer solutions (pH from 4.5 to 6.5; see Experimental procedures). The samples were excited at 340 and 380 nm in an inverted microscope and the emission intensity was measured at 530 nm (Figure 8a).

Due to the fact that the central vacuole occupies most of the volume of leaf cells and protoplasts, the measurement of fluorescence emission from SAVs was affected by the contribution of a strong fluorescent signal from the central vacuole. To overcome this problem, we isolated vacuoplasts (central vacuole surrounded by plasma membrane) and miniplasts (protoplast with no central vacuole but containing

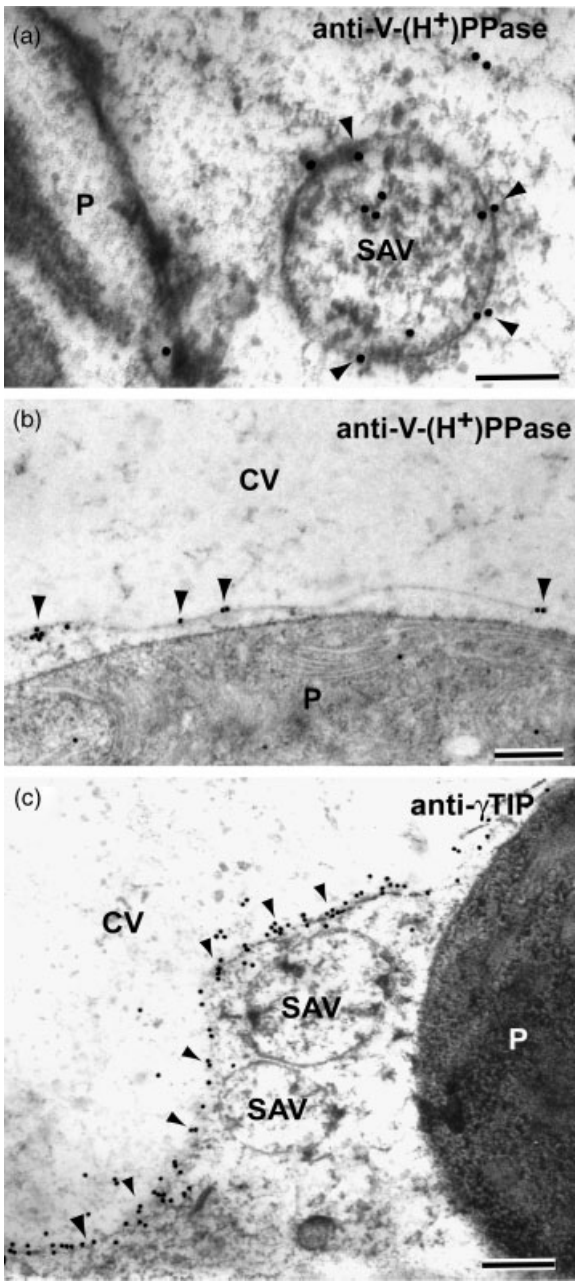


**Figure 4.** Immunolocalization of vacuolar markers in senescing Arabidopsis leaf cells.
(a, b) Immunolabeling of the Arabidopsis vacuolar ($H^+$)-pyrophosphatase. Note the positive labeling on the tonoplast of both senescence-associated vacuoles (SAVs; a) and central vacuole (CV; b) indicated by arrowheads.
(c) Immunolabeling of γ-TIP VM23. Note that the tonoplast of the central vacuole is heavily labeled whereas the tonoplast of SAVs is not.
P, plastid. Scale bar = 250 nm.

SAVs) from senescing Arabidopsis leaves (see Experimental procedures) and incubated them in Lysosensor Yellow/Blue (Figure 8b–e). The ratio $I_{340/380}$ obtained after subtracting the background signal was significantly higher in vacuoplasts (2.51 ± 0.31) than in miniplasts (1.8 ± 0.27). According to the calibration curve, the values correspond to lumenal pH values of 6 for the central vacuole and 5.2 for SAVs.

### *SAVs are present in leaves of the atapg7-1 mutant*

Because SAVs appear to contain partially degraded cellular material in their lumen, and autophagy-related genes have been shown to be upregulated during leaf senescence in Arabidopsis (Doelling *et al.*, 2002; Hanaoka *et al.*, 2002), we evaluated whether SAVs might originate by autophagy. In yeast, APG7 is involved in two autophagic mechanisms, that is the APG8 and APG12 conjugation pathways, both required for autophagosome formation (Khalfan and Klionsky, 2002). The *atapg7-1* mutant has been recently characterized and shows an accelerated senescence phenotype (Doelling *et al.*, 2002). Therefore, we chose this mutant to test for the presence of SAVs. We incubated protoplasts from senescing leaves of *atapg7-1* plants with R-6502 and Lysotracker Red. In both cases, we detected a punctuate fluorescent pattern similar to that observed in wild-type senescing leaf cells (data not shown). These results indicate that AtAPG7 is not required for SAV formation, although an autophagic origin of SAVs mediated by an APG7-independent pathway cannot be ruled out.

### *The Arabidopsis sag12-2 mutant shows no altered senescence phenotype*

To determine the specific function of SAG12 during leaf senescence, we searched an Arabidopsis T-DNA mutant collection (Arabidopsis Knockout Facility, http://www.biotech.wisc.edu/Arabidopsis) for insertions affecting *SAG12*. We identified one allele, *sag12-2*, which contains a T-DNA insertion in the second exon (Figure 9a). As shown in Figure 9(b), *SAG12* transcripts could not be detected in the homozygous *sag12-2* mutant, whereas the levels of transcripts from other SAG genes such as *SAG13* did not differ from WT plants, confirming that only *SAG12* expression was specifically impaired.

Despite the absence of *SAG12* transcripts, homozygous *sag12-2* mutants showed no visibly altered phenotype during senescence compared with WT plants (Figure 9c). Moreover, SAVs with proteolytic activity were detected in senescing leaves of the *sag12-2* mutant (data not shown), indicating that SAG12 is not required for SAV formation and that other Cys proteases in addition to SAG12 accumulate in this vacuolar compartment.

## Discussion

### *Senescing leaf cells contain two types of lytic vacuoles*

We have found that during leaf senescence, small vacuoles of around 550–700 nm in diameter develop in the peripheral

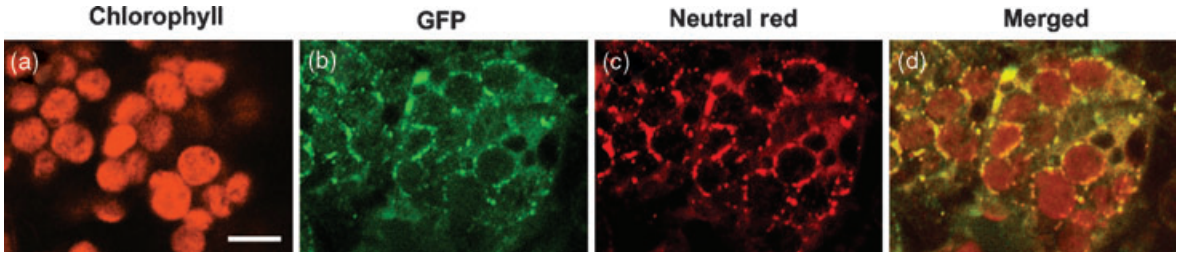


**Figure 5.** SAG12-GFP localization in senescing Arabidopsis leaves.
Confocal images (1 μm section) through the mesophyll of a senescing leaf (S2) from a *SAG12-GFP* transgenic plant incubated with Neutral Red. Note that the GFP signal colocalizes with the fluorescence from Neutral Red (d), indicating that SAG12-GFP is inside a vacuolar compartment.
Scale bar in (a)–(d) = 10 μm.

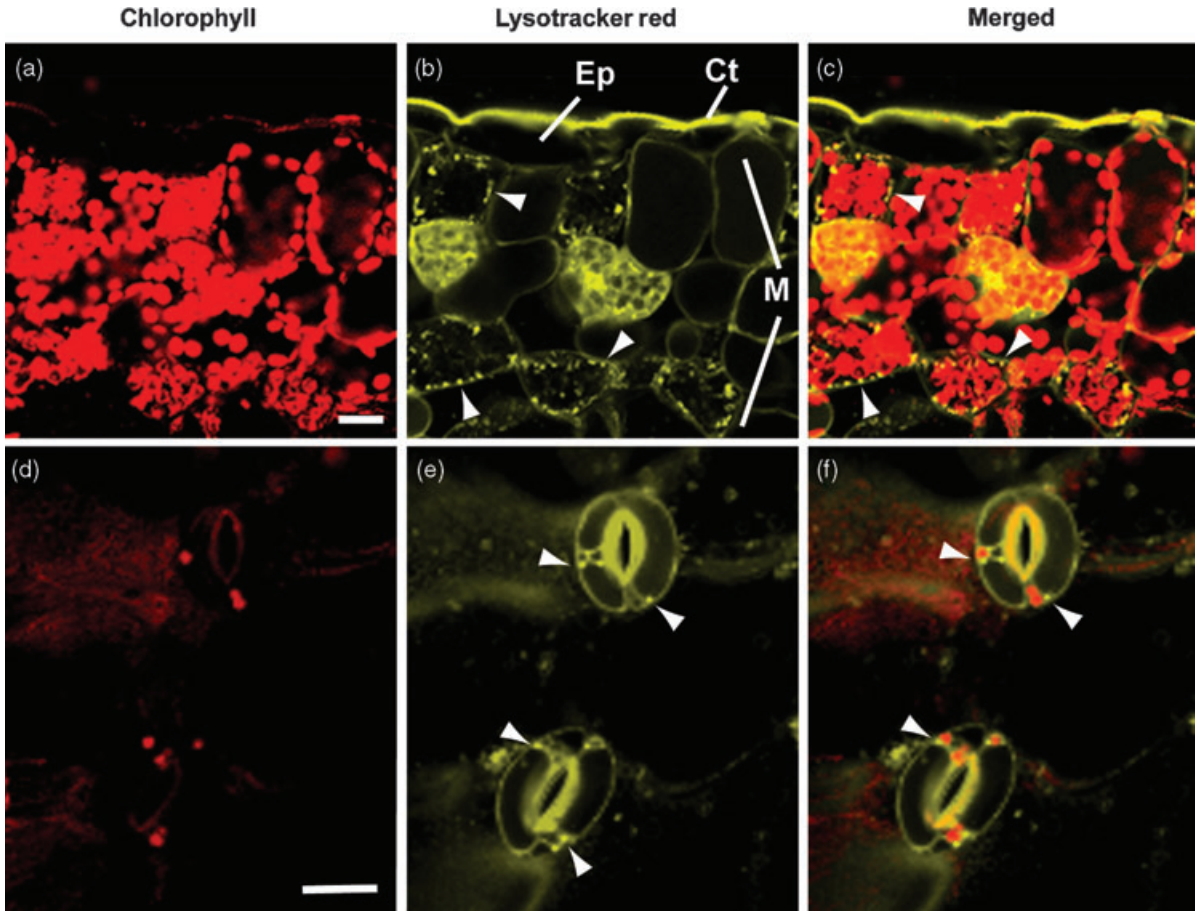


**Figure 6.** Senescence-associated vacuole (SAV) distribution in senescing Arabidopsis leaves.
(a–c) Confocal images (1 μm section) through a senescing leaf (S2) incubated with Lysotracker Red. Note the fluorescent punctuate pattern of the Lysotracker Red signal corresponding to SAVs in mesophyll (M) cells (b, c). The cuticle layer (Ct) has been stained by the dye and shows a high non-specific fluorescent signal. Ep, epidermis.
(d–f) Confocal images (1 μm section) through the epidermis of a senescing leaf (S2) incubated with Lysotracker Red.
Scale bars = 20 μm.

cytoplasm of cells that contain chloroplasts, that is, mesophyll and guard cells. We have concluded that these organelles are vacuoles based on their ability to sequester Neutral Red, Lysotracker Red and Lysosensor Yellow/Blue, and on their positive labeling with antibodies against the V-($H^+$)-pyrophosphatase. Because these organelles arise during senescence, we have called them SAVs. We have also determined that SAVs exhibit an intense Cys-protease activity and accumulate SAG12-GFP. Moreover, SAG12 expression in the leaf appears to be limited to those cells that

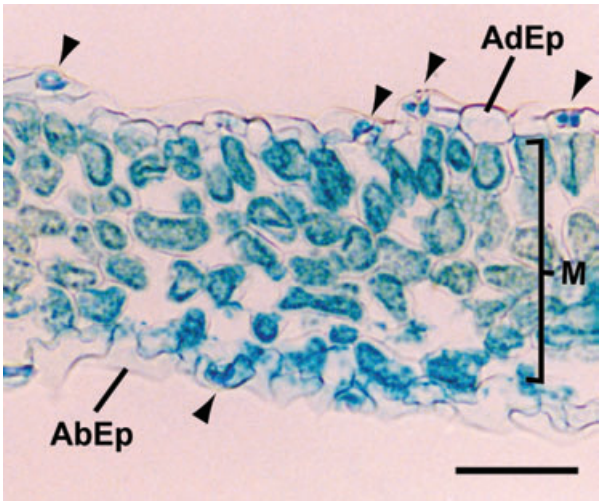


**Figure 7.** *Pro*$_{SAG12}$*:GUS* expression in senescing Arabidopsis leaves.
Senescing leaf (S1) samples from transgenic plants harboring the *Pro*$_{SAG12}$*:GUS* construct incubated for 20 h in X-Gluc substrate show expression in mesophyll (M) and guard cells (arrowheads). AdEp, adaxial epidermis; AbEp, abaxial epidermis.
Scale bar = 50 μm.

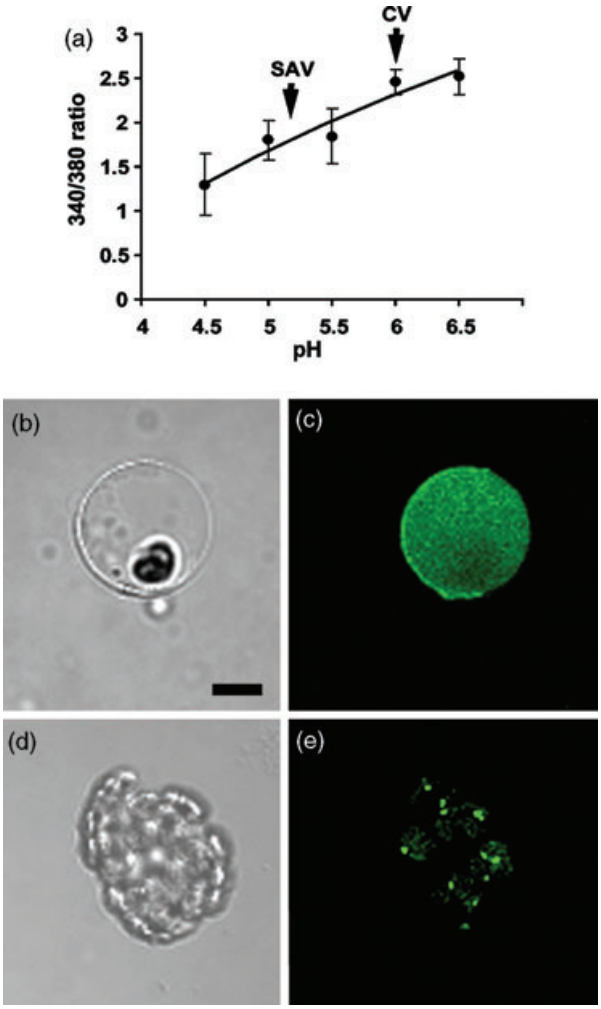


**Figure 8.** Ratiometric fluorescence determination of lumenal pH in isolated vacuoplasts and miniplasts from senescing Arabidopsis leaves loaded with Lysosensor Yellow/Blue.
(a) Calibration curve.
(b, c) Isolated vacuoplasts observed using differential interference contrast (DIC) optics (b) and 488-nm excitation in a confocal microscope (c). The fluorescence signal comes from the central vacuole.
(d, e) Isolated miniplasts observed as in (b) and (c), respectively. The fluorescence signal comes from the senescence-associated vacuoles (SAVs).
Scale bar = 10 μm.

develop SAVs, that is, chloroplast-containing cells. In addition, we have shown that SAVs are more acidic than the central vacuole and that the SAV tonoplast membrane differs in aquaporin composition from the tonoplast of the central vacuole.

These results imply that two distinct types of vacuoles coexist in most senescing leaf cells, for example the SAVs and the central vacuole. A comparable scenario has been described in other plant systems such as barley aleurone cells, which also undergo programmed cell death and exhibit two types of vacuoles: the protein storage vacuoles and the smaller, lysosome-like 'secondary vacuoles' (Swanson *et al.*, 1998). Interestingly, it has been proposed that the secondary vacuoles are involved in autophagy and the death of the aleurone cells (Swanson *et al.*, 1998). Secondary vacuoles may be related to the aleurain-containing vacuoles reported previously (Holwerda and Rogers, 1992), although this hypothesis remains to be proved.

The presence of two types of vacuoles in the aleurone system makes biological sense. Protein storage vacuoles are storage compartments, and secondary vacuoles may be lytic compartments. However, the presence of two types of lytic vacuoles in senescing leaf cells is harder to explain. Some of the results presented in this study may shed light on this issue. First, we have shown that SAVs lack the aquaporin γ-TIP, which is present in the tonoplast of the central vacuole. This means that the identity of the tonoplast of both vacuoles is different and thus, the regulation of transport across the tonoplast could also differ in both of them. Second, SAVs are more acidic than the central vacuole. Although we cannot determine at this point if SAVs and the central vacuole differ in their protease composition, the existence of different intravacuolar pH values suggests that the proteolytic activity between the two compartments could vary qualitatively and quantitatively, for example, by providing appropriate environments to proteases with different pH optima. *In vivo* manipulation of vacuolar pH has shown that increases of 0.5–0.65 units are enough to greatly reduce protein degradation in vacuoles of *Chara* (Moriyasu, 1995) and barley aleurone cells (Hwang *et al.*, 2003), implying that the 0.8 pH unit difference between SAVs and the central vacuole can be quite significant in terms of protease activity. Thus, the central vacuole and the SAVs could differ

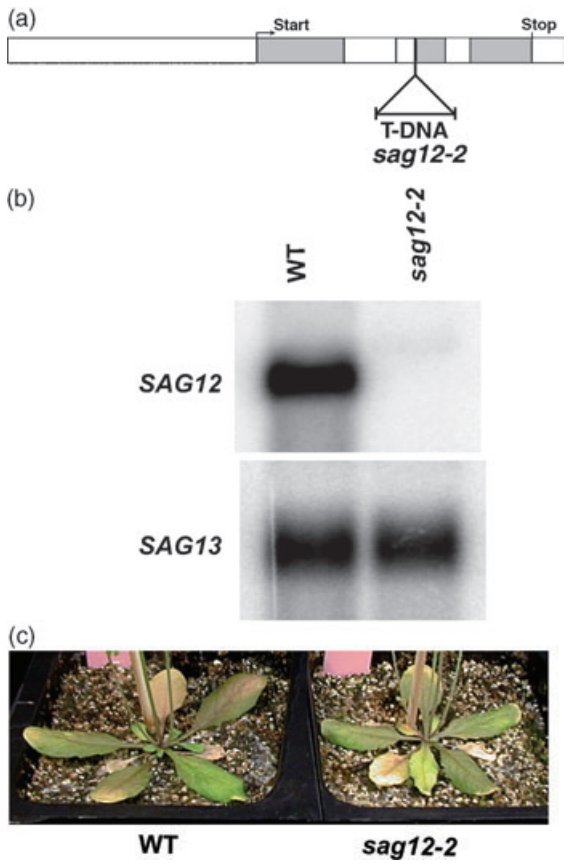


**Figure 9.** *SAG12-2* knockout mutant.
(a) T-DNA insertion in the second exon of *SAG12* in *sag12-2*. Gray boxes indicate translated exons, and white boxes indicate 5′ and 3′ untranslated regions and introns.
(b) *SAG12* expression in wild type (WT; ecotype Ws) and *sag12-2*. RNA was isolated from fully senescing leaves of Arabidopsis grown in long days (16 h of light and 8 h of dark). The blot was probed first with *SAG12* and then reprobed with *SAG13* (Lohman *et al.*, 1994) as a control.
(c) Normal progression of leaf senescence in *sag12-2*. The picture shows *sag12-2* plants grown for 29 days in long-day conditions. Compared with WT, *sag12-2* did not display any noticeable phenotypic differences including senescence progression. The same phenotypes were observed in short days (8 h of light and 16 h dark; data not shown).

enough to provide distinct lytic environments for dismantling specific cellular components.

### *The senescence-associated Cys-protease SAG12 fused to GFP localizes to the SAVs*

Arabidopsis *SAG12* encodes a papain-like Cys-protease, which is expressed specifically during leaf senescence. Based on its amino acid sequence, SAG12 is predicted to be targeted to the secretory pathway (TARGETP 1.0; Emanuelsson *et al.*, 2000), and to have an N-terminal signal peptide (SignalP V1.1; Nielsen *et al.*, 1997). In this study, we have found that the fusion protein SAG12-GFP expressed in Arabidopsis transgenic plants under the control of the $Pro_{SAG12}$ is targeted to SAVs.

Whereas GFP has been widely used to visualize many different types of organelles in plants, observation of GFP targeted to lytic vacuoles in whole plants entails some difficulties (Neuhaus, 2000). Accordingly, whereas the $Pro_{SAG12}$ has been shown to be strongly active during leaf senescence (Noh and Amasino, 1999a), the GFP signal in SAVs of $Pro_{SAG12}$:*SAG12-GFP* transgenic plants was notably low. This result could be due to the fact that either the green fluorescent signal can be attenuated by protonation of the fluorophore of GFP in the acidic lumen of vacuoles or, as it has been shown recently, GFP could be rapidly degraded inside plant vacuoles. (Flückiger *et al.*, 2003; Tamura *et al.*, 2003). Transfer of transgenic plants to the dark for 1–2 days before observation avoids the light-dependent degradation of GFP in vacuoles of non-senescing tissues (Tamura *et al.*, 2003). However, we do not observe variation in GFP fluorescence in relation to different light conditions. If the intense Cys-proteolytic activity detected inside SAVs is degrading GFP molecules, it does not seem to be attenuated by dark conditions.

### *SAV development and SAG12 expression occur simultaneously in chloroplast-containing leaf cells*

Based on the analysis of both high-pressure frozen/freeze-substituted leaf samples by electron microscopy and leaf pieces loaded with fluorescent vacuolar markers, we have demonstrated that SAVs develop in mesophyll and guard cells of S1, S2, and S3 leaves but not in other leaf cells that do not contain chloroplasts. In addition, the analysis of *SAG12:GUS* plants clearly shows that SAG12 expression in senescing leaves is restricted to mesophyll and guard cells and occurs simultaneously with SAV formation.

Although we have not yet determined the function of SAG12-containing SAVs, it is tempting to speculate that they could be involved in the degradation of molecules released from chloroplasts as they are present only in chloroplast-containing leaf cells. The mechanism of degradation of chloroplast proteins during senescence has not been completely elucidated. Whereas some level of proteolytic activity has been detected in intact chloroplasts (Ragster and Chrispeels, 1981), most of the proteases and lipases which increase during senescence appear to be targeted to the vacuole (Feller and Fisher, 1994; Wittenbach *et al.*, 1982; Yamada *et al.*, 2001). In fact, several lines of evidence suggest that peptides and catabolites generated inside the chloroplast are released from chloroplasts and further metabolized elsewhere in the leaf cells (Hörstensteiner and Feller, 2002). We have failed to immunolocalize epitopes from chloroplastic proteins inside SAVs (data not shown), but the absence of labeling could simply reflect an intense degradation of the substrates in this vacuolar compartment.

Alternatively, SAVs could be specialized lytic compartments for the dismantling of cytoplasmic components in chloroplast-containing leaf cells.

### *Cys-proteases and Cys-protease-containing compartments are involved in other known cases of programmed cell death in plants*

Programmed cell death has been described in a variety of plant developmental processes and the expression pattern of certain Cys-proteases, either by upregulation or specific expression, has been considered as a marker of the plant cell death program (Swidzinski *et al.*, 2002). For example, the differentiation of the inner integument in *Brassica napus* seeds (Wan *et al.*, 2002), the formation of tracheary elements in Arabidopsis (Funk *et al.*, 2002), and the senescence of the aleurone tissue during seed germination are associated with the specific expression or upregulation of both papain-like and aleurain-like Cys-proteases.

A papain-like group of Cys proteases with a KDEL motif is expressed in several senescing tissues, especially in seed tissues during germination. The inactive precursors of these Cys-proteases accumulate in ER-derived organelles, called ricinosomes in the castor bean endosperm (Schmid *et al.*, 2001) and KDEL vesicles in *Vigna mungo* (Toyooka *et al.*, 2000). After fusion of the ER-derived compartments with the vacuole, the proteases become active by removal of their pro-peptides. ER-derived organelles containing precursors of two Cys-proteases, RD21 and the vacuolar processing enzyme VPE$\gamma$, both with no known ER retention signal, have been identified in *A. thaliana* seedlings (Hayashi *et al.*, 2001; Rojo *et al.*, 2003). These ER bodies are thought to be involved in cell death induced by stress and/or senescence. These observations indicate that Cys-proteases stored in ER-derived compartments in senescing tissues reach the vacuole bypassing the Golgi apparatus. From a structural point of view, the protease precursor compartments derived from the ER are easily identified in the electron microscope by the presence of attached ribosomes on their surface. Interestingly, we have not detected any cellular structure in our senescing leaf samples that could resemble an ER-derived precursor protease compartment, suggesting that Cys-proteases in senescing leaf cells follow a different pathway to the vacuole, probably involving the Golgi compartment.

Leaves express a variety of Cys-proteases during senescence. Arabidopsis SAG12 is special in that it is specifically expressed during senescence, whereas other Cys-proteases such as SAG2/ATALEU, VPE$\gamma$, and RD21 are expressed in young leaves and are additionally upregulated during senescence (Buchanan-Wollaston, 1997; Gepstein *et al.*, 2003; Kinoshita *et al.*, 1999; Yamada *et al.*, 2001). However, the absence of an altered senescence phenotype in the *sag12-2* Arabidopsis mutant clearly demonstrates that SAG12 is not required for the visual progression of senescence. In addition, the detection of Cys-proteolytic activity in SAVs of *sag12-2* suggests that other proteases, besides SAG12, are targeted to this compartment.

In plants, vacuoles can be formed from fragmentation of other vacuoles, from the ER, from the *trans*-Golgi network, or by autophagic mechanisms (Marty, 1999). Although we have not detected early SAV-formation intermediates that could help to precise the origin of SAVs, the following considerations would seem to provide constraints on the possible mechanisms involved in their formation. First, the absence of $\gamma$-TIP in the SAV tonoplast suggests that SAVs do not derive from fragmentation of the central vacuole, which shows a tonoplast highly enriched in this aquaporin. Second, although the dense appearance of SAV contents resemble those of autophagic compartments, the presence of functional SAVs in the *apg7* mutant clearly indicates that APG7, which is necessary for autophagosome assembly (Khalfan and Klionsky, 2002), is not involved in SAV formation. Thus, SAVs could arise by an APG7-independent autophagic pathway or could be derived from specific ER domains.

We are currently focusing on the isolation of SAVs and the identification of the proteases and substrates contained in this vacuolar compartment to determine the specific function of this organelle during leaf senescence.

## Experimental procedures

### *Plant material and growth conditions*

*Arabidopsis thaliana* (ecotypes Columbia, Col, and Wassilewskija, Ws) was grown in soil with Arabidopsis controlled-release fertilizer (Lehle Seeds, Round Rock, TX, USA). Plants were grown at 23°C with an 11-h-light/13-h-dark cycle. Arabidopsis *apg7*mutant plants (Doelling *et al.*, 2002), the *sag12-2* T-DNA insertional mutant plants, and transgenic plants harboring the $Pro_{SAG12}$:*SAG12-GFP* construct were in Ws, whereas the $Pro_{SAG12}$:*GUS* construct (pSAG12P-1345) was expressed in Col (Noh and Amasino, 1999a).

Soybean (*Glycine max*) cv. Clark seeds were obtained from the USDA Northern Germoplasm Collection (Department of Agronomy, University of Illinois, Urbana, IL, USA). Plants were grown in a chamber at 26°C day/21°C night, at 450 $\mu$m $m^{-2}$ $sec^{-1}$ irradiance, and with a 10-h-light/14-h-dark cycle.

### *Plasmid construction and plant transformation*

To make the $Pro_{SAG12}$:*SAG12-GFP* construct, 4.3 kb genomic DNA containing 2.8 kb 5′ upstream region and entire exon and intron sequence of *SAG12* was amplified by PCR using 12GFP1 (5′-AC**CCATGG**CTCCTATAGTTGGGTAAGAAGCTTTCATGGC-3′) and 12GFP2 (5′-GC**GAGCTC**TCGACAAGCTATAGACCTCAAG-3′) as primers; restriction sites are shown in boldface, and sequences corresponding to the *SAG12* region are underlined. The resulting PCR product was digested with *Sac*I-*Nco*I and ligated to the *Sac*I-*Nco*I-digested pAVA393 (von Arnim *et al.*, 1998), resulting in pNA127. In pNA127, *SAG12* was translationally fused to *GFP* through a three-amino-acid linker (IAG), which was inserted in the place of the *SAG12* stop codon and right before the start codon of

*GFP*. 5.2 kb *Sac*I-*Pst*I fragment from pNA127 containing *SAG12-GFP-terminator* was subcloned into *Sac*I-*Pst*I-digested pPZP221, resulting in pNA128. Arabidopsis (ecotype Ws) plants were transformed with pNA128-containing *Agrobacterium tumefaciens* strain ABI by infiltration (Clough and Bent, 1998). Transgenic lines were selected on agar-solidified medium containing 0.65 g $l^{-1}$ Peter's Excel 15-5-15 fertilizer (Scotts, Maysville, OH, USA) and 50 μg $ml^{-1}$ gentamycin.

### *Isolation of sag12-2*

*sag12-2* was isolated from the Kan population of the Arabidopsis Knockout Facility (http://www.biotech.wisc.edu/Arabidopsis/) by a PCR-based reverse genetic approach (Krysan *et al.*, 1996) using 12KO-1 (5′-GCAAAACATCATCAACACATATCCAACTTCG-3′) or 12KO-2 (5′-TTTTAGACATCAATCCCACACAAACATACAC-3′) as gene-specific primers and JL202 (5′-CATTTTATAATAACGCTGCG-GACATCTAC-3′) as a left border T-DNA-specific primer. A single T-DNA insertion in the second exon of *SAG12* between sequences 5′-TGCGACACAA-3′ and 5′-ACGATTTTGG-3′ was confirmed by the single-gene segregation of kanamycin resistance and by the sequencing of the T-DNA borders.

### *RNA gel blot analysis*

Total RNA was isolated using TRI Reagent (Sigma, St Louis, MO, USA) according to the manufacturer's instructions. For RNA gel blots, 20 μg of total RNA was separated by denaturing formaldehyde-agarose gel electrophoresis as described by Sambrook *et al.* (1989). Full-length cDNA fragments were used as *SAG12* and *SAG13* probes.

### *Quantification of chlorophyll*

Chlorophyll content was estimated by taking measurements at the center of the leaves with a Minolta SPAD-502 chlorophyll meter (Osaka, Japan).

### *Preparation of protoplasts and isolated cells from Arabidopsis and soybean leaves*

Non-senescing and senescing leaves of *A. thaliana* and soybean were cut into small pieces with a razor blade and incubated in suspension buffer (0.6 M manitol, 0.1% w/v BSA, 20 mM MES pH 6) for 30 min, under vacuum and in darkness. The leaf pieces were then incubated in digestion buffer (1% cellulase, 0.3% pectinase, 0.3% driselase, 0.5 M manitol, 0.1% w/v BSA, 20 mM MES pH 5.8 for Arabidopsis and 1% pectinase, 0.5 M manitol, 0.1% w/v BSA, 20 mM MES pH 5.8 for soybean) at room temperature with gentle shaking for 2 h. Arabidopsis protoplasts and isolated leaf cells from soybean were separated from undigested tissue fragments by filtration through a 100-μm mesh and collected by centrifugation at 50 ***g*** for 15 min at room temperature. Protoplasts and isolated cells were gently resuspended in suspension buffer. Cellulase, pectinase and driselase were purchased from Sigma.

### *Fluorescent probes*

Lysotracker Red DND-99, Lysosensor Yellow/Blue DND-160, and the Cys-protease substrate R-6502 were purchased from Molecular Probes (Eugene, OR, USA) and Neutral Red from Sigma. Both Lysotracker Red DND-99 and Lysosensor Yellow/Blue DND-160 were kept as 1 mM stock solutions in DMSO. R-6502 was kept as a 5-mM stock solution in DMF.

### *Laser scanning confocal microscopy*

Protoplasts, isolated cells and leaf pieces were incubated with 1% Neutral Red (15 min), 5 μM Lysotracker Red (10 min), and 50 μM R-6502 (20 min) (Molecular Probes). After washing the excess of dye, samples were observed in a LSM 510 laser scanning confocal microscope (Carl Zeiss, Oberkochen, Germany). GFP and R-6502 were excited with the 488-nm line of an argon laser and the emission was monitored using a 505–550-nm bandpass filter. Lysotracker Red and Neutral Red were excited with the 543 nm helium-neon laser line and imaged through a 560–605 nm bandpass filter; whereas chlorophyll detection was achieved by using a 633-nm line for excitation and a 650-nm longpass filter for emission.

Images were acquired using the Zeiss LSM Image Examiner Version 2.30.011. Colocalization images were obtained using the same software after parallel confocal image acquisition. For further processing, images were imported as TIF files into Adobe Photoshop 6.0.1 (Mountain View, CA, USA).

### *Ratiometric estimation of intravacuolar pH*

The pH calibration curve was obtained according to Diwu *et al.* (1999) with modifications. Leaf protoplasts were incubated in 20 μM Lysosensor Yellow/Blue DND-160 [2-(4-pyridyl)-5-(4-(2-dimethylaminoethylamino-carbamoyl)-methoxy)-phenyl-oxazole, Molecular Probes] for 1 h. The excess of dye was removed by washing protoplasts with 20 mM MES, 0.45 M betaine buffer (pH6). Then, protoplasts were treated with MES calibration buffers (10 mM MES, 0.45 M betaine), ranging from pH 4.5 to 6.5, and containing 10 μM nigericin (Sigma). Measurements were taken 5–10 min after addition of nigericin. Protoplasts were visualized in an inverted microscope (Nikon Diaphot 200, Tokyo, Japan) adapted for epifluorescence, excited at 340 and 380 nm, and the fluorescence emission intensity was recorded at 530 nm. The intensity ratio ($I_{340/380}$) was calculated after subtracting the background signal.

To determine the fluorescence emission of SAVs and central vacuoles, we obtained vacuoplasts and miniplasts from protoplasts of Arabidopsis senescing leaves according to Yamada *et al.* (2001) with modifications. Protoplasts were layered on a Percoll gradient consisting of 2 ml of 60% Percoll (v/v) (Sigma) and 2.5 ml of 30% Percoll in 10 mM MES (pH 6), 0.5 M betaine, and 10 mM $CaCl_2$. A 0.5 ml volume of the same solution with no Percoll was added on top of the Percoll suspension and the gradient was centrifuged at 10 000 ***g*** for 1 h using a swing out rotor (MLS 50; Beckman Instruments, Palo Alto, CA, USA). Vacuoplasts and isolated central vacuoles were collected from the upper fraction whereas miniplasts (protoplasts with no central vacuole) were collected in the 60–30% Percoll interphase. Then, vacuoplasts and miniplasts were incubated in 20 μM Lysosensor Yellow/Blue for 1 h and the fluorescence emission intensity ratios ($I_{340/380}$) were calculated separately for each of them in the same way as explained above for intact protoplasts, with the exception that samples were kept in 20 mM MES, 0.45 M betaine buffer (pH 6) and no nigericin was added.

The fluorescence emission intensity ratios ($I_{340/380}$) obtained from vacuoplasts and miniplasts were converted to absolute values of vacuolar pH by comparison with the calibration curve. Tukey's test

was used to analyze ratiometric values and $P < 0.05$ was taken to indicate statistical significance.

### *GUS histochemical analysis*

Histochemical staining for GUS activity was performed according to Jefferson *et al.* (1987). Small pieces of senescing leaves from plants expressing the $Pro_{SAG12}$:*GUS* construct (pSAG12P-1345; Noh and Amasino, 1999a) were vacuum-infiltrated and incubated with a solution containing 2 mM 5-bromo-4-chloro-3-indolyl-β-D-glucopyranoside (Sigma), 50 mM $NaPO_4$ buffer (pH 7.2), 50 mM $K_3Fe(CN)_6$, and 50 mM $K_4Fe(CN)_6$ at 37°C for 20 h. Then, samples were dehydrated, embedded in Paraplast (Oxford Labware, St Louis, MO, USA), and sectioned.

### *Electron microscopy*

Arabidopsis and soybean leaves were sectioned with a razor blade into small pieces and infiltrated with hexadecane. Leaf samples were then loaded in sample holders filled with hexadecene, frozen in a Baltec HPM 010 high-pressure freezer (Technotrade, Manchester, NH, USA), and transferred to liquid nitrogen for storage. Substitution was performed in 2% $OsO_4$ in anhydrous acetone at −80°C for 72 h, and followed by slow warming to room temperature over a period of 2 days. After several acetone rinses, samples were teased from the holders and infiltrated in Epon resin (Ted Pella Inc., Redding, CA, USA) following the schedule: 5% resin in acetone (4 h), 10% resin (12 h), 25% resin (12 h) 50, 75, and 100% (24 h each concentration). Polymerization was carried out at 60°C. Sections were stained with 2% uranyl actetate in 70% methanol for 10 min followed by Reynold's lead citrate (2.6% lead nitrate and 3.5% sodium citrate, pH 12) and observed in a Zeiss EM 109.

For immunolabeling, some high-pressure frozen samples were substituted in 0.1% uranyl acetate plus 0.2% glutaraldehyde in acetone at −80°C for 72 h, and warmed to −50°C for 24 h. After several acetone rinses these samples were infiltrated with Lowicryl HM20 (Electron Microscopy Sciences, Fort Washington, PA, USA) for 72 h and polymerized at −50°C under UV light for 72 h. Sections were mounted on formvar-coated nickel grids and blocked for 20 min with a 5% (w/v) solution of non-fat milk in PBST (0.1% Tween-20). The antibodies anti-V-($H^+$)-pyrophosphatase, and anti-VM23 (Maeshima, 1992) were applied for 1 h at room temperature. The sections were rinsed in a stream of PBST (0.5% Tween-20) and then transferred to the secondary antibody (anti-rabbit IgG 1:50 in PBST) conjugated to 15 nm gold particles for 1 h. Controls were performed by omitting the primary antibody.

Upon request, materials integral to the findings presented in this publication will be made available in a timely manner to all investigators on similar terms for non-commercial research purposes. To obtain SAG12 lines contact Richard M. Amasino, amasino@biochem.wisc.edu

## Acknowledgements

We thank Tomas Santa Coloma (Fundación Instituto Leloir, Buenos Aires, Argentina) for the use of the confocal microscope, Masayoshi Maeshima (Nagoya University, Nagoya, Japan) for providing us with the anti-VM23 and anti V-($H^+$)-pyrophosphatase antibodies, and Alicia Mattiazzi (Facultad de Medicina, Universidad Nacional de La Plata, La Plata, Argentina) for the use of the equipment for pH determination. We also thank Jotham R. Austin, II for his valuable comments on the manuscript. This work was supported by a grant (PIP 0327) from CONICET (Consejo Nacional de Investigaciones Científicas y Técnicas) to J.J.G., a grant (14022-14) from Antorchas Foundation to M.S.O, and an NIH grant GM61306 to LAS. The work of R.M.A. and Y.-S.N was supported by the College of Agricultural and Life Sciences and the Graduate School of the University of Wisconsin, and by the United States–Israel BARD grant 3326-02C. The creation of insertion mutant lines was supported by National Science Foundation grant 0116945. M.S.O. and M.G.V.P. are CONICET researchers. JJG is a CICBA researcher.

## References

**von Arnim, A.G., Deng, X.W. and Stacey, M.G.** (1998) Cloning vectors for the expression of green fluorescent protein fusion proteins in transgenic plants. *Gene*, **221**, 35–43.

**Buchanan-Wollaston, V.** (1997) The molecular biology of leaf senescence. *J. Exp. Bot.* **48**, 181–199.

**Buchanan-Wollaston, V. and Ainsworth, C.** (1997) Leaf senescence in *Brassica napus*. *Plant Mol. Biol.* **33**, 821–834.

**Clough, S.J. and Bent, A.F.** (1998) Floral dip: a simplified method for *Agrobacterium*-mediated transformation of *Arabidopsis thaliana*. *Plant J.* **16**, 735–743.

**De, D.N.** (2000) *Plant Cell Vacuoles. An Introduction*. Collingwood, Australia: CSIRO Publishing.

**Di Sansebastiano, G.P., Paris, N., Marc-Martin, S. and Neuhaus, J.-M.** (2001) Regeneration of a lytic central vacuole and of neutral peripheral vacuoles can be visualized by green fluorescent proteins targeted to either type of vacuoles. *Plant Physiol.* **126**, 78–86.

**Diwu, Z., Chen, C.-S., Zhang, C., Klaubert, D.H. and Haugland, R.P.** (1999) A novel acidotropic pH indicator and its potential application in labeling acidic organelles of live cells. *Chem. Biol.* **6**, 411–418.

**Doelling, J.H., Walker, J.M., Friedman, E.M., Thompson, A.R. and Vierstra, R.D.** (2002) The APG8/12-activating enzyme APG7 is required for proper nutrient recycling and senescence in *Arabidopsis thaliana*. *J. Biol. Chem.* **277**, 33105–33114.

**Drake, R., John, I., Farrell, A., Cooper, W., Schuch, W. and Grierson, D.** (1996) Isolation and analysis of cDNAs encoding tomato cysteine proteases expressed during leaf senescence. *Plant Mol. Biol.* **30**, 755–767.

**Emanuelsson, O., Nielsen, H., Brunak, S. and von Heijne, G.** (2000) Predicting subcellular localization of proteins based on their N-terminal amino acid sequence. *J. Mol. Biol.* **300**, 1005–1016.

**Eskelinen, E.-L., Prescott, A.R., Cooper, J., Brachmann, S.M., Wang, L., Tang, X., Backer, J.M. and Lucocq, J.M.** (2002) Inhibition of autophagy in mitotic animal cells. *Traffic*, **3**, 878–893.

**Feller, U. and Fisher, A.** (1994) Nitrogen metabolism in senescing leaves. *Crit. Rev. Plant Sci.* **13**, 241–273.

**Flückiger, R., De Caroli, M., Piro, G., Dalessandro, G., Neuhaus, J.-M. and Di Sansebastiano, G.P.** (2003) Vacuolar system distribution in *Arabidopsis* tissues, visualized using GFP fusion proteins. *J. Exp. Bot.* **54**, 1577–1584.

**Funk, V., Kositsup, B., Zhao, C. and Beers, E.P.** (2002) The Arabidopsis xylem peptidase XCP1 is a tracheary element vacuolar protein that may be a papain ortholog. *Plant Physiol.* **128**, 84–94.

**Gan, S. and Amasino, R.M.** (1995) Inhibition of leaf senescence by autoregulated production of cytokinin. *Science*, **270**, 1966–1967.

**Geisler, M., Frangne, N., Gomès, E., Martinoia, E. and Palmgren, M.** (2000) The *ACA4* gene of Arabidopsis encodes a vacuolar membrane calcium pump that improves salt tolerance in yeast. *Plant Physiol.* **124**, 1814–1827.

**Gepstein, S., Sabehi, G., Carp, M.-J., Hajouj, T., Nesher, M.F.O., Yariv, I., Dor, C. and Bassani, M.** (2003) Large-scale identification of leaf senescence-associated genes. *Plant J.* **36**, 629–642.

**Hanaoka, H., Noda, T., Shirano, Y., Kato, T., Hayashi, H., Shibata, D., Tabata, S. and Oshumi, Y.** (2002) Leaf senescence and starvation-induced chlorosis are accelerated by the disruption of an Arabidopsis autophagy gene. *Plant Physiol.* **129**, 1181–1193.

**Hayashi, H., Yamada, K., Shimada, T., Matsushima, R., Nishizawa, N.K., Nishimura, M. and Hara-Nishimura, I.** (2001) A proteinase-storing body that prepares for cell death or stresses in the epidermal cells of Arabidopsis. *Plant Cell Physiol.* **42**, 894–899.

**Holopainen, J.M., Saarikoski, J., Kinnunen, P.K.J. and Järvelä, I.** (2001) Elevated lysosomal pH in neuronal ceroid lipofuscinoses (NCLs). *Eur. J. Biochem.* **298**, 5851–5856.

**Holwerda, B.C. and Rogers, J.C.** (1992) Purification and characterization of aleurain. *Plant Physiol.* **99**, 848–855.

**Hörstensteiner, S. and Feller, U.** (2002) Nitrogen metabolism and remobilization during senescence. *J. Exp. Bot.* **53**, 927–937.

**Hwang, Y.-S., Bethke, P.C., Gubler, F. and Jones, R.L.** (2003) cPrG-HCl a potential $H^+/Cl^-$ symporter prevents acidification of storage vacuoles γ aleurone cells and inhibits GA-dependent hydrolysis of storage protein and phytate. *Plant J.* **35**, 154–163.

**Jauh, G.Y., Philips, T.E. and Rogers, J.C.** (1999) Tonoplast intrinsic protein isoforms as markers for vacuolar functions. *Plant Cell*, **11**, 1867–1882.

**Jefferson, R.A., Kavanagh, T.A. and Bevan, M.W.** (1987) GUS fusion: β-Glucuronidase as a sensitive and versatile gene fusion marker in higher plants. *EMBO J.* **6**, 3901–3907.

**Khalfan, W.A. and Klionsky, D.J.** (2002) Molecular machinery required for autophagy and the cytoplasm to vacuole targeting (Cvt) pathway in *S. cerevisiae*. *Curr. Opin. Cell Biol.* **14**, 468–475.

**Kinoshita, T., Yamada, K., Hiraiwa, N., Nishimura, M. and Hara-Nishimura, I.** (1999) Vacuolar processing enzymes are upregulated in the lytic vacuoles of vegetative tissues during senescence and under various stressed conditions. *Plant J.* **19**, 43–53.

**Krysan, P.J., Young, J.C., Tax, F. and Sussman, M.R.** (1996) Identification of transferred DNA insertions within *Arabidopsis* genes involved in signal transduction and ion transport. *Proc. Natl Acad. Sci. USA*, **93**, 8145–8150.

**Lim, P.O., Woo, H.R. and Nam, H.G.** (2003) Molecular genetics of leaf senescence in *Arabidopsis*. *Trends Plant Sci.* **8**, 272–278.

**Lin, J.-F. and Wu, S.-H.** (2004) Molecular events in senescing *Arabidopsis* leaves. *Plant J.* **39**, 612–628.

**Lohman, K.N., Gan, S., John, M.C. and Amasino, R.M.** (1994) Molecular analysis of natural leaf senescence in *Arabidopsis thaliana*. *Physiol. Plant.* **92**, 322–328.

**Maeshima, M.** (1992) Characterization of the major integral protein of vacuolar membrane. *Plant Physiol.* **98**, 1248–1254.

**Marty, F.** (1999) Plant vacuoles. *Plant Cell*, **11**, 587–599.

**Matile, P.** (1975) *The Lytic Compartment of Plant Cells*. Wien, Germany: Springer-Verlag.

**Minamikawa, T., Toyooka, K., Okamoto, T., Hara-Nishimura, I. and Nishimura, M.** (2001) Degradation of 1,5-bisphosphate carboxylase/oxygenase by vacuolar enzymes of senescing French bean leaves: immunocytochemical and ultrastructural observation. *Protoplasma*, **218**, 144–153.

**Moriyasu, Y.** (1995) Examination of the contribution of vacuolar proteases to intracellular protein degradation in *Chara corallina*. *Plant Physiol.* **109**, 1309–1315.

**Moriyasu, Y. and Hillmer, S.** (2000) Autophagy and vacuole formation. In *Vacuolar Compartments* (Robinson, D.G. and Rogers, J.C., eds). Boca Raton, FL: CRC Press, pp. 71–89.

**Nakabayashi, K., Ito, M., Kiyosue, T., Shinozaki, K. and Watanabe, A.** (1999) Identification of *clp* genes expressed in senescing *Arabidopsis* leaves. *Plant Cell Physiol.* **40**, 504–514.

**Neuhaus, J.-M.** (2000) GFP as a marker for vacuoles in plants. In *Vacuolar Compartments* (Robinson, D.G. and Rogers, J.C., eds). Boca Raton, FL: CRC Press, pp. 254–269.

**Nielsen, H., Engelbrecht, J., Brunak, S. and von Heijne, G.** (1997) Identification of prokaryotic and eukaryotic signal peptides and prediction of their cleavage sites. *Protein Eng.* **10**, 1–6.

**Noh, Y.-S. and Amasino, R.M.** (1999a) Identification of the promoter region responsible for the senescence-specific expression of *SAG12*. *Plant Mol. Biol.* **41**, 181–194.

**Noh, Y.-S. and Amasino, R.M.** (1999b) Regulation of developmental senescence is conserved between *Arabidopsis* and *Brassica napus*. *Plant Mol. Biol.* **41**, 195–206.

**Noodén, L.D. and Guiamet, J.J.** (1996) Genetic control of senescence and aging in plants. In *Handbook of the Biology of Aging* (Schneider, E.L. and Rowe, J.W., eds). San Diego, CA: Academic Press, pp. 94–118.

**Paris, N., Stanley, C.M., Jones, R.L. and Rogers, J.C.** (1996) Plant cells contain two functionally distinct vacuolar compartments. *Cell*, **85**, 563–572.

**Quirino, B.F., Noh, Y.-S., Himelblau, E. and Amasino, R.M.** (2000) Molecular aspects of leaf senescence. *Trends Plant Sci.* **5**, 278–282.

**Ragster, L.E. and Chrispeels, M.J.** (1981) Autodigestion in crude extracts of soybean leaves and isolated chloroplasts as a measure of proteolytic activity. *Plant Physiol.* **67**, 104–109.

**Robinson, D.G. and Hinz, G.** (1997) Vacuole biogenesis and protein transport to the plant vacuole: a comparison with the yeast vacuole and the mammalian lysosome. *Protoplasma*, **197**, 1–25.

**Rojo, E., Zouhar, J., Carter, C., Kovaleva, V. and Raikhel, N.V.** (2003) A unique mechanism for protein processing and degradation in *Arabidopsis thaliana*. *Proc. Natl Acad. Sci. USA*, **100**, 7389–7394.

**Sambrook, J., Fritsch, E.F. and Maniatis, T.** (1989) *Molecular Cloning: A Laboratory Manual*. Cold Spring Harbor, NY: Cold Spring Harbor Laboratory Press.

**Schmid, M., Simpson, D.J., Sarioglu, H., Lottspeich, F. and Gietl, C.** (2001) The ricinosome of senescing plant tissue bud from the endoplasmic reticulum. *Proc. Natl Acad. Sci. USA*, **98**, 5353–5358.

**Smart, C.M., Hosken, S.E., Thomas, H., Greaves, J.A., Blair, B.G. and Schuch, W.** (1995) The timing of maize leaf senescence and characterization of senescence-related cDNAs. *Physiol. Plant.* **93**, 673–682.

**Swanson, S.J., Bethke, P.C. and Jones, R.L.** (1998) Barley aleurone cells contain two types of vacuoles: characterization of lytic organelles by use of fluorescent probes. *Plant Cell*, **10**, 685–698.

**Swidzinski, J.A., Sweetlove, L.J. and Leaver, C.J.** (2002) A custom microarray analysis of gene expression during programmed cell death in *Arabidopsis thaliana*. *Plant J.* **30**, 431–446.

**Tamura, K., Shimada, T., Ono, E., Tanaka, Y., Nagatani, A., Higashi, S., Watanabe, M., Nishimura, M. and Hara-Nishimura, I.** (2003) Why green fluorescent fusion proteins have not been observed in the vacuoles of higher plants. *Plant J.* **35**, 545–555.

**Toyooka, K., Okamoto, T. and Minamikawa, T.** (2000) Mass transport of a proform of a KDEL-tailed cysteine proteinase (SH-EP) to protein storage vacuoles by endoplasmic reticulum-derived vesicles is involved in protein mobilization in germinating seeds. *J. Cell Biol.* **148**, 453–463.

**Toyooka, K., Okamoto, T. and Minamikawa, T.** (2001) Cotyledon cells of *Vigna mungo* seedlings use at least two distinct autophagic machineries for degradation of starch granules and cellular components. *J. Cell Biol.* **154**, 973–982.

**Wan, L., Xia, Q., Qiu, X. and Selvaraj, G.** (2002) Early stages of seed development in *Brassica napus*: a seed coat-specific cysteine proteinase associated with programmed cell death of the inner integument. *Plant J.* **30**, 1–10.

**Weaver, L.M., Gan, S., Quirino, B.F. and Amasino, R.M.** (1998) A comparison of the expression patterns of several senescence-associated genes in response to stress and hormone treatment. *Plant Mol. Biol.* **37**, 455–469.

**Wittenbach, V.A., Lin, W. and Hebert, R.R.** (1982) Vacuolar localization of proteases and degradation of chloroplasts in mesophyll protoplasts from senescing primary wheat leaves. *Plant Physiol.* **69**, 98–102.

**Yamada, K., Matsushima, R., Nishimura, M. and Hara-Nishimura, I.** (2001) A slow maturation of a cysteine protease with granulin domain in the vacuoles of senescing Arabidopsis leaves. *Plant Physiol.* **127**, 1626–1634.